Controlled Release of Nanoparticles and Macromolecules from Responsive Microgel Capsules

Hassan Masoud and Alexander Alexeev*

George W. Woodruff School of Mechanical Engineering, Georgia Institute of Technology, Atlanta, Georgia 30332, United States

ABSTRACT

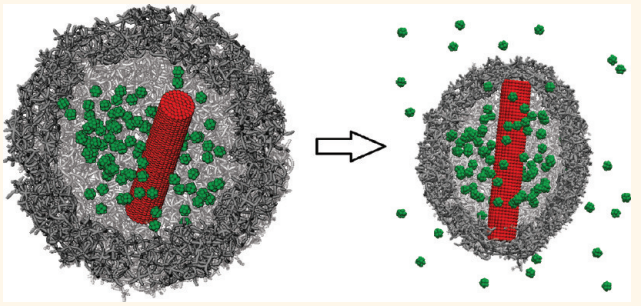

Using a mesoscale computational model, we probe the release of nanoparticles and linear macromolecules from hollow microgel capsules that swell and deswell in response to external stimuli. Our simulations reveal that responsive microcapsules can be effectively utilized for steady and pulsatile release of encapsulated solutes. Swollen gel capsules allow steady, diffusive release of nanoparticles and polymer chains, whereas gel deswelling causes burst-like discharge of solutes driven by an outward flow of the solvent enclosed within a shrinking capsule. We demonstrate that this hydrodynamic release can be regulated by introducing rigid microscopic rods in the capsule interior. Thus, our findings disclose an efficient approach for controlled release from stimuli-responsive microcarriers that could be useful for designing advanced drug delivery systems.

KEYWORDS: responsive hydrogel capsule · controlled release · drug delivery · polymer network · volume transition · dissipative particle dynamics

Water-swellable polymer networks (hydrogels) that are sensitive to external stimuli have found an increasingly large number of applications in optoelectronics, nanotechnology, microelectromechanical systems, and nanomedicine.[1−6] Triggered by external stimuli, such as variations in temperature, pH, solvent composition, light intensity, and magnetic and electrical fields, hydrogels can absorb solvent (swell) or expel solvent (deswell), and, as a result, change their volume by many times.[7−11] Their high sensitivity to the environmental changes makes hydrogels especially attractive for drug delivery applications, in which delivery agents can effectively shield and protect the encapsulated drugs until they reach a treatment site, and then discharge a predefined amount of the drug, thereby playing an active role in disease therapy.[12] Indeed, researchers have successfully exploited polymer gels to create responsive micro- and nanodelivery agents that can release encapsulated drugs or other solutes on demand.[12−21]

Despite notable recent progress in synthesis and characterization of micro/nano gels, the development of multifunctional delivery carriers remains to be a challenge. The release from microscopic gel carriers usually involves multiple time and length scales, geometrical complexities, and tight coupling between mechanical and fluid processes within the gel polymer network,[22−24] which make it difficult not only to rationally design experiments, but also to develop theoretical models able to predict the dynamic behavior of these multicomponent responsive systems.

Herein, we introduce a mesoscale computational model of responsive hydrogels, that is, chemically cross-linked networks of elastic polymer filaments immersed in a Newtonian fluid. Our model is based on dissipative particle dynamics (DPD) and can explicitly capture the transport of nanoscopic solutes within responsive polymer networks with complex geometries and associated fluid flows (Figure 1). This allows us, for the first time, to directly probe the release dynamics of nanoparticles and linear polymer chains from the interior of hollow gel microcapsules during swelling and deswelling volume transitions (Figure 2).

Our simulations reveal that capsule swelling results in a steady diffusive release, whereas gel deswelling induces a burst-like discharge of encapsulated nanoparticles and macromolecules. In the latter case, the fast release of encapsulated solutes is facilitated

* Address correspondence to alexander.alexeev@me.gatech.edu.

Received for review September 2, 2011 and accepted December 16, 2011.

Published online December 16, 2011
10.1021/nn2043143

by an outward flow of the solvent initially enclosed in the shrinking gel capsule, which rapidly transports solutes through membrane pores. The amount of hydrodynamically discharged solutes can be regulated by the degree of deswelling and by introducing micrometer-sized rods inside the capsule that mitigate membrane sealing by stretching it. Furthermore, we demonstrate that periodically deswelling capsules can be effectively harnessed in applications that require multipulse release characterized by alternating periods of fast release and periods of no release.

RESULTS AND DISCUSSION

We load gel microcapsules with linear macromolecules (Figure 1a) and nanoscopic particles (Figure 1b) that are initially uniformly distributed in the capsule interior and probe their release when the capsules undergo swelling and deswelling (Figure 2). When gel swells and the polymer network expands, the capsule increases in size and the external solvent penetrates into the growing capsule interior, whereas gel deswelling leads to capsule shrinking and, consequently, a part of the encapsulated solvent is expelled through the porous gel membrane. This cross-membrane flow defines the dynamics of the capsule volume change, which can be described in terms of a force balance between mechanical stresses in the elastic gel network which undergoes volume transition and viscous stresses due to the cross-membrane fluid flow.[25,26]

We first probe the release of nanoparticles and macromolecules from capsules in the initial equilibrium state which is characterized by membrane porosity $\varepsilon \approx 0.85$ (Figure 1). Figure 3 shows the cumulative fraction of released solutes as a function of release time. Here, time is normalized by the characteristic time of capsule volume transition $\tau_c = R_i^2/9D_0$, where R_i is the capsule outer radius in the initial state and D_0 is the coefficient of collective diffusion of the gel.[25] For capsules considered in our study, $D_0 \approx 0.065$ leading to $\tau_c \approx 400$ (see Supporting Information). In Figure 3, each point represents an average over five independent realizations. We find that only a few particles and chains can diffuse out of the shell during the simulation time. This slow release is due to a small network mesh size in the initial capsule that suppresses the diffusion of solutes across the shell.

In Figure 4, we show the cumulative size distributions of membrane pores of the capsule in its initial equilibrium and in the swollen and deswollen states.[27,28] Here, the pore size is estimated as the radius of the largest circle contained in a triangle formed by three adjacent network filaments and nondimensionalized by the particle radius R_p. Indeed, we find that the average pore size in the initial equilibrium is smaller than the particle radius R_p and the chain radius of gyration $R_g \approx 1.4R_p$. In these conditions, the solute diffusion rate in the network is orders of magnitude slower than in the pure solvent.[29]

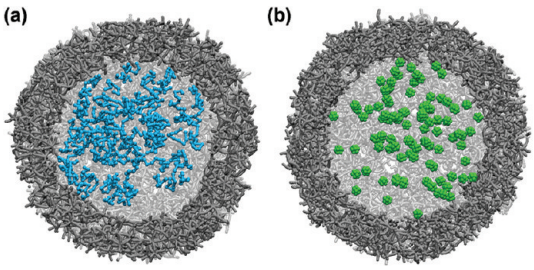

Figure 1. Cross-sectional views of initially equilibrated hollow spherical capsules loaded with (a) polymer chains (cyan) and (b) nanoparticles (green) inside the capsule cavity. The shell porosity is $\varepsilon = 0.85$ and the thickness is $b = R_i/3$, where R_i is the initial outer radius of the capsule. For clarity, solvent is not shown.

When the gel swells, the network expands and both the capsule diameter and thickness increase by approximately 50% (Figure 2a,b)[30] leading to porosity $\varepsilon \approx 0.95$ and larger membrane pores (Figure 4a,c). While the porosity increases by only 10% from the initial capsule state, the solute diffusivity in the membrane, which is an exponential function of ε,[31,32] increases by an order of magnitude.[29] This significant change of the shell diffusivity enables a steady release of encapsulated nanoparticles and macromolecules (Figure 3). We find an approximately 10-fold increase in the release rate compared to the release from the initial capsule, indicating that the release is controlled by the membrane diffusivity.

This diffusion driven release for both nanoparticles and macromolecules proceeds with a nearly constant rate as indicated by a linear change in the cumulative number of released solutes in time (Figure 3). The rate of chain release is roughly twice slower than that of particles that have a smaller characteristic size and, therefore, can more easily percolate through an expanded gel network.[33,34]

This constant release rate has been previously observed in experiments that probed the diffusion of solutes encapsulated in hollow microcapsules.[35−38] For example, Kono *et al.*[38] studied the release of NaCl from pH-responsive polyamide capsules and showed that the NaCl release is linearly related to time. The diffusive release has been also studied theoretically by considering particle diffusion through a porous capsule shell.[39] The long time solution predicts a release with a constant rate that is defined by the capsule geometry and the particle diffusion through the capsule shell. Thus, our simulation of release from swollen capsules agrees well with both experiment and theory.

When the capsule deswells, its diameter and membrane thickness decreases by 20% compared to the initial capsule size (Figure 2c,d) resulting in a smaller membrane pore size (Figures 4a,d). In this situation, one might expect that solute release will be further suppressed. Surprisingly, we found that it is not the case for hollow microgel capsules, where a rapid and

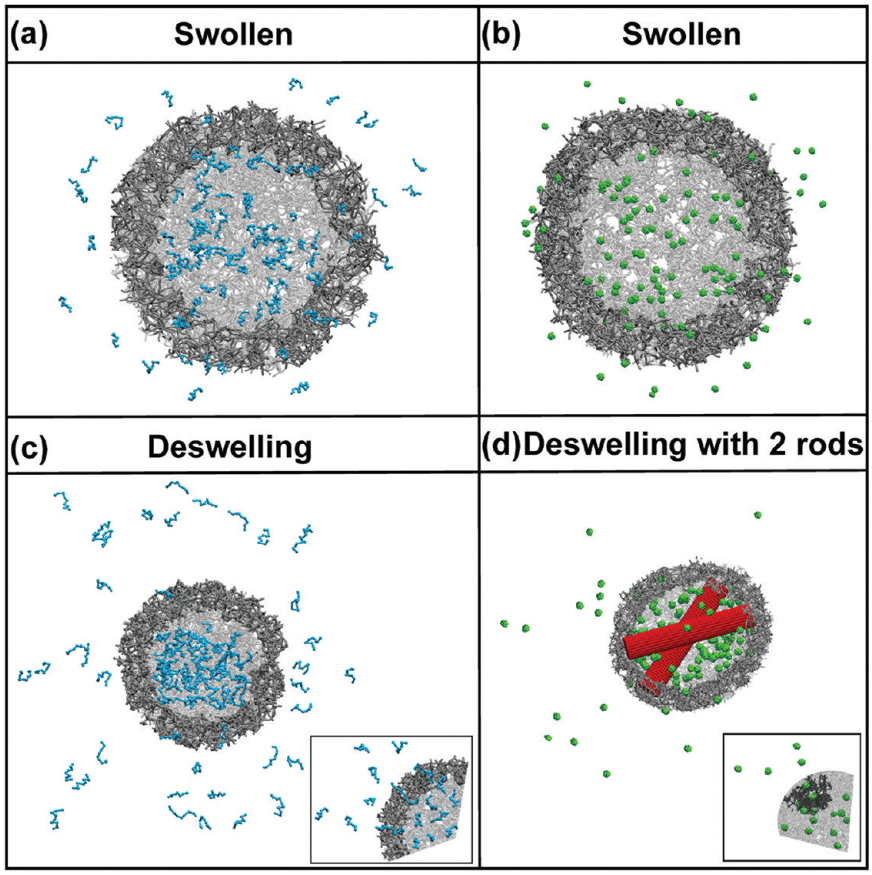

Figure 2. Panels a and b are snapshots from our simulations illustrating the release from swollen gel capsules of, respectively, encapsulated polymer chains (cyan) and nanoparticles (green). The swollen capsules have an outer radius $1.5R_i$ and porosity $\varepsilon = 0.95$. Panels c and d are snapshots illustrating the release of, respectively, polymer chains and nanoparticles during capsule deswelling. The deswollen capsules have an outer radius $0.8R_i$ and porosity $\varepsilon = 0.75$. Panel c shows the release from a hollow capsule without rods, whereas panel d shows the release from a capsule with two enclosed microrods (red). The rods are not connected to each other and can move freely inside the cavity of an initially equilibrated capsule. For clarity, cross sections of the capsules are shown, whereas solvent is not shown. The inset in panel c shows polymer reptation across the deswelling capsule membrane. The inset in panel d shows a stream of nanoparticles discharging through a membrane pore during deswelling.

massive release takes place during the capsule deswelling (Figure 3). This release is characterized by a rate which is much faster than that from swollen capsules with larger pores (*cf.* Figures 4c,d). Furthermore, we found that during deswelling polymer chains are released nearly twice faster than nanoparticles and the total amount of released chains is about four times greater (remember that the chains have a nearly 50% larger characteristic size than the nanoparticles and the release rate of chains from swollen capsules is about twice slower than that of nanoparticles). This fast solute release, however, only occurs for a short period during which the capsule undergoes the volume change.

Contrary to the swollen gel capsules where the release is controlled by diffusion, the release from deswelling capsules is facilitated by convective fluid flows induced by capsule shrinking. When capsule volume decreases, the encapsulated fluid is squeezed out from the capsule interior, carrying suspended solutes and enabling their rapid release. Since larger pores in the capsule shell have lower hydrodynamic resistance, the encapsulated solvent flows through these larger pores, which allows the release even when the pore size decreases due to gel deswelling. The insets in Figure 2c,d illustrate the release of nanoparticles and polymer chains discharged through pores in a deswelling membrane.

We can estimate the efficacy of the hydrodynamic release by introducing a dimensionless Peclet number $Pe = ub/D_n$ that compares the characteristic rate of solute discharge due to the fluid flow during capsule deswelling with the rate of diffusion from an unswollen capsule. Here, D_n is the effective diffusion coefficient of solutes in the capsule membrane network in the initial state, b is the membrane thickness, and $u = \Delta V/(4\pi\tau_c(R_i - b)^2)$ is the characteristic volume flow rate of encapsulated fluid per unit membrane area, where $\Delta V = {}^4/_3\pi(R_i - b)^3(1 - \alpha^3)$ is the change in the capsule internal volume during deswelling and $\alpha = R_f/R_i$ is the deswelling ratio with R_f being the final outer radius.

Using the above expressions, we find that the Peclet number $Pe = 3(1 - \alpha^3)(D_0/D_n)\,(b(R_i - b)/R_i^2)$. Here, the

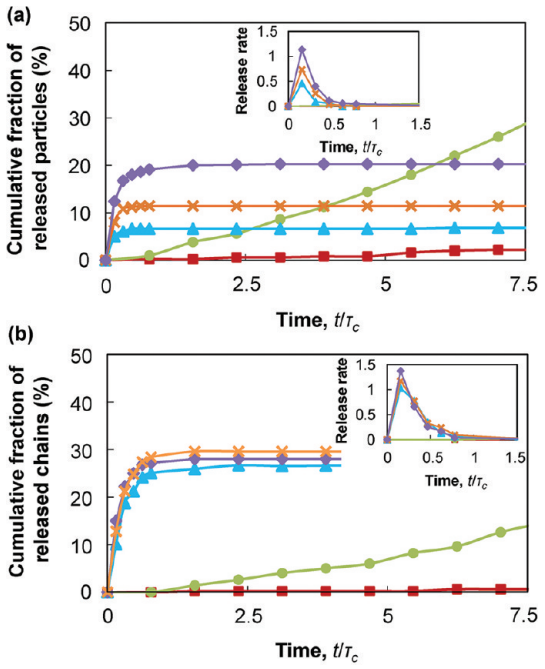

Figure 3. Cumulative fraction of (a) released nanoparticles and (b) released polymer chains *versus* time. The insets show the dimensionless release rate as a function of time. The squares, circles, triangles, crosses, and diamonds are for, respectively, initially equilibrated capsules, swelling capsules, deswelling capsules, and deswelling capsules with one rod and two rods. Each point is an average of five independent realizations.

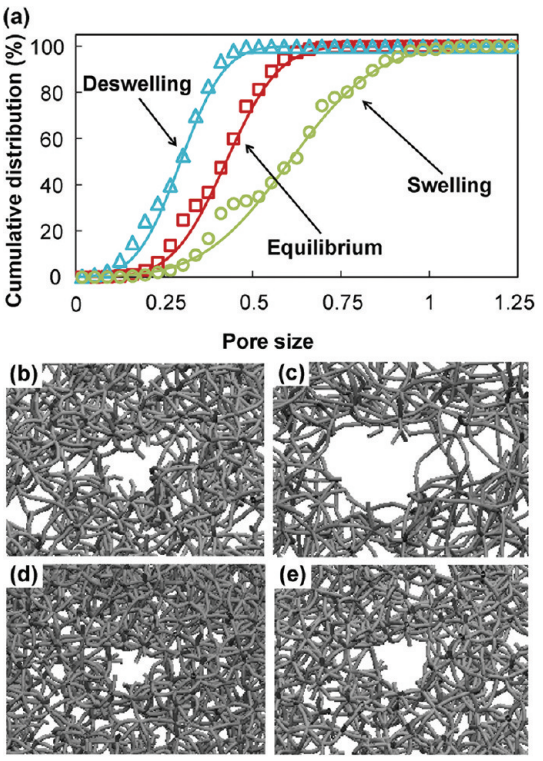

Figure 4. Panel a shows cumulative pore size distribution of the capsule shell formed from a random network of interconnected filaments. The pore size is nondimensionalized by nanoparticles radius R_p. The symbols represent simulation data and the solid lines represent fits of normal distributions with the average and standard deviations identical to those of the simulation data. Panels b–e show representative changes in the pore size of the capsule membrane in the initial equilibrium, swollen, deswollen, and deswollen with two enclosed microrods states, respectively.

first term indicates that convective transport is enhanced when the deswelling ratio decreases and more internal fluid is released. The second term represents the ratio between the capsule collective diffusion and the solute diffusion, and shows that the effect of hydrodynamic release can be enhanced by faster volume transition (larger D_0) and/or slower solute diffusion rate (smaller D_n). The last term represents the effect of capsule geometry and indicates that the hydrodynamic release is increased when the shell thickness is $b \approx 0.5R_i$.

For our simulation parameters, *Pe* is equal to about 120 and 450 for nanoparticles and polymer chains, respectively. Here, we estimate the effective diffusion coefficient D_n based on the release data shown in Figure 3. We find that our scaling model agrees well with the simulation results for polymer chains in which case $Pe \approx 420$. However, when it comes to nanoparticles, our simulations yield $Pe \approx 30$. Thus, the model predicts the number of hydrodynamically released particles about four times greater than what we obtain in the simulations.

This discrepancy between the scaling model and our simulations of nanoparticle release can be attributed to the rapid decrease of membrane pore size in shrinking capsules. When pores become too small for rigid particles to pass, the release terminates even when the encapsulated solvent is still leaking from inside the capsule. Indeed, we find that the nanoparticle release stops after $t/\tau_c \approx 0.5$, whereas the release of compliant polymer chains that can easily reptate through the porous membrane continues approximately twice longer driven by an outward fluid flow.

To prevent membrane sealing due to pore shrinking in deswelling capsules and to enhance the release of nanoparticles, we introduce rigid microrods in the capsule interior (Figure 2d). The rods are comparable in length with the internal capsule diameter and can freely move inside an initially unswollen capsule. However, when the capsule shrinks and decreases in size, the rods resist capsule shrinkage and stretch the membrane. The mechanical stretching induces stresses in the membrane that oppose the network contraction due to gel deswelling, thereby keeping the membrane pores open (Figure 4e).

The cumulative release and the release rates for deswelling microcapsules with one and two internal rods are shown in Figure 3. Indeed, we find that rigid rods enhance the discharge rate of rigid nanoparticles compared to both the deswelling capsules without internal rods and the diffusion-controlled release from

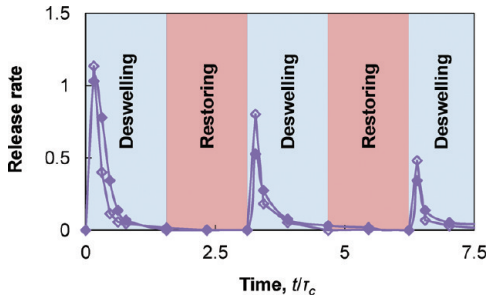

Figure 5. Pulsatile release from hollow responsive microcapsules that undergo reversible deswelling/restoring cycles. Filled symbols show a dimensionless release rate of polymer chains from a capsule without rods (see Figure 2c). Empty symbols show dimensionless release rate of nanoparticles from a capsule with two encapsulated microrods (see Figure 2d). Each deswelling and restoring interval equals to $t/\tau_c = 1.6$.

the swollen capsules (Figure 3a). Furthermore, we find that the net release of particles from a capsule with two separate rods is almost twice greater than from a capsule with one internal rod, and results in $Pe \approx 90$, which is close to the theoretical limit. We relate this additional release enhancement to a stronger membrane stretching by two internal rods compared to one rod. Thus, by changing the number of encapsulated microrods one can engineer nanoparticle-loaded capsules that yield different release rates.

Whereas the release of nanoparticles is very sensitive to the presence of encapsulated microrods, the release of polymer chains from deswelling capsules remains practically unaffected after the inclusion of the rods (Figure 3b). The difference in the amount of released chains for simulations without rods and for simulations with one and two rods does not exceed 10%. This confirms that the release of linear macromolecules is not limited by the pore sealing in deswelling gel, but rather by the amount of released solvent during the capsule volume change.

Gels can typically swell and deswell reversibly[40−42] which makes responsive gels especially attractive for applications where periods of rapid discharge of encapsulated solutes should be followed by intervals of no release.[43,44] Such pulsatile drug delivery systems, for example, can be utilized in biomedical settings in which a precise amount of the drug should be administrated with specific time intervals.[45]

To probe the utility of responsive microcapsules in multipulse release applications, we carry out simulations of periodic release of macromolecules from capsules without rods and nanoparticles from capsules that enclose two independent rigid rods. In these simulations, capsules cyclically deswell (Figure 2c,d) and restore their initial state (Figure 1a,b) with constant time intervals equal to $1.6\tau_c$. Figure 5 shows the release profiles during three successive capsule deswelling/restoring cycles. The simulations reveal that immediately after the beginning of a deswelling interval, a significant amount of solutes is released. This burst release is then followed by a period of no release, which continues until the beginning of the next capsule deswelling period. Thus, the released amount is defined by the dynamics of capsule deswelling and is insensitive to a particular extent of deswollen and swollen periods if they are greater than τ_c. The total amount of solutes that are released in consecutive cycles decreases due to their decreasing concentration within the periodically deswelling capsules.

The phenomena predicted in our simulations can be experimentally realized using microgel capsules with the outer radius of the order of 1 μm and the collective diffusion coefficient $D_0 \approx 10^{-7}-10^{-8}$ cm^2/s. Responsive capsules with such properties can be prepared using a verity of experimental techniques.[12,15,18,19,25,46−49] For instance, Zha *et al.*[46] and Xing *et al.*[19] synthesized temperature responsive nanogel capsules by colloidal template polymerization followed by core removal. Zhang *et al.*[47] prepared responsive hollow nanogel shells by synthesizing core−shell nanogels. A hollow capsule was obtained after the degraded core was released through the shell. Wahrmund *et al.*[25] employed a capillary-based microfluidic device to form monodisperse poly-*N*-isopropylacrylamide (PNIPAM) hydrogel microcapsules. Another microfluidic approach was developed by Seiffert *et al.*[15] to synthesize multilayered microgel capsules. A variety of stimuli responsive micro- and nanocapsules can also be formed using layer-by-layer (LbL) techniques.[18,50]

To induce a controlled release, these responsive capsules need to be loaded with nanoparticles and polymer chains with characteristic sizes comparable to the average pore size of the gel network which is typically in the range from tens to hundreds of nanometers. For example, Zahr *et al.*[51] used LbL assembly to encapsulate drug nanoparticles inside a macromolecular nanoshell. Wang *et al.*[52] introduced a facile approach for encapsulating water-insoluble compounds in polymer capsules using mesoporous silica particle-mediated drug loading followed by the generation of a polymer multilayer shell using the LbL technique. Kozlovskaya *et al.*[53] fabricated hydrogel capsules by hydrogen-bonded self-assembly and then used them to encapsulate FITC-dextran by locking the capsule wall with electrostatically associating polycations at high pH.

Microencapsulation techniques are not limited to nanometer-sized solutes. Experiments have shown that micrometer-sized large structures can also be encapsulated inside the capsules. Kim *et al.*[54] and Shum *et al.*[55] demonstrated that microfluidics can be effectively employed to encapsulate objects comparable to the container in size. Dahne *et al.*[56] and Vriezema *et al.*[57] showed that large objects can be self-assembled or polymerized inside microcapsules. Such approaches can be potentially employed to encapsulate microrods inside responsive gel capsules.

The amount of solute release from experimental microgel capsules can be adjusted by changing gel porosity and the degree of gel swelling/deswelling. Furthermore, the release time from deswelling capsules can be directly regulated by changing the capsule relaxation time τ_c. Since this time scale is proportional to R^2, the use of smaller capsules enables faster release. For example, for a capsule with typical network diffusivity $D_0 \approx 10^{-7}$ cm^2/s, the release time of the order of seconds can be obtained if the capsule radius is about a few micrometers.

CONCLUSION

We introduced a coarse-grained computational method that can explicitly capture the release of nanoparticles and macromolecules from responsive microgel capsules. Our simulations revealed that not only swelling, but also deswelling of hollow microcapsules can be harnessed for controlled release. Indeed, recent experiments with poly(acrylic acid) (PAA) and poly(*N*-isopropylacrylamide) (PNIPAM) hollow nanogels demonstrated the possibility of solute release from deswelling microcapsules.[58] We showed that the release mechanisms for swollen and deswelling gel capsules are different. The release from swollen capsules is relatively slow, controlled by the solute diffusion through the capsule shell. The rate of this release depends on the degree of capsule swelling that sets the membrane porosity and, therefore, can be tuned in a wide range by modifying the gel chemistry. The release from deswelling capsules, on the other hand, is burst-like and is driven by the flow of the encapsulated solvent triggered by capsule shrinking. This rapid and massive hydrodynamic release occurs on the time scale of the deswelling volume transition. The amount of released solutes is controlled by the capsule volume decrease, whereas the release rate is defined by the deswelling kinetics. We found that deformable polymer chains that can easily penetrate thorough membrane pores are released in larger amounts from deswelling capsules than are nanoparticles that are filtered out by shrinking membrane pores. Our simulations further demonstrated that the inclusion of rigid microrods inside deswelling capsules mitigates the membrane pore closing, and in this fashion provides an effective method for regulating the rate of hydrodynamic release of nanoparticles. Finally, we showed that the periodic deswelling of responsive capsules can be utilized in multipulse release applications. Thus, responsive microcapsules offer a uniquely adaptive and tunable means of delivery that provides effective mechanisms for both basal and pulsatile release of encapsulated drugs and other solutes.

METHODS

To explicitly model the complex dynamic interactions among a responsive microgel capsule, a viscous fluid, and encapsulated diffusive nanoparticles and polymer chains, we use dissipative particle dynamics (DPD),[59,60] a coarse-grained simulation technique that employs a momentum-conserving thermostat and soft repulsive interactions among beads representing clusters of molecules. This method allows for the simulation of physical phenomena occurring at relatively large time and spatial scales, while accurately capturing the relevant hydrodynamic effects. Indeed, DPD has been successfully employed to simulate the dynamics of polymers and particles dispersed in Newtonian incompressible fluids.[29,61−69]

In DPD, the time evolution of the many-body system obeys Newton's second law $m\,d\mathbf{v}_i/dt = \mathbf{f}_i$, where $\mathbf{v}_i$ and $\mathbf{f}_i$ are, respectively, the velocity and force on the ith bead with mass m at time t. The equations of motion are integrated using the velocity-Verlet algorithm.[60] The force on the bead i is $\mathbf{f}_i = \sum_j(\mathbf{F}^C_{ij} + \mathbf{F}^D_{ij} + \mathbf{F}^R_{ij})$, where the sum runs over all neighbor beads j within a cutoff radius r_c around bead i. The conservative force is given by $\mathbf{F}^C_{ij} = a_{ij}(1 - \hat{r}_{ij})\,\hat{\mathbf{r}}_{ij}$, where a_{ij} is the repulsion between beads i and j, $\hat{r}_{ij} = r_{ij}/r_c$, and $\hat{\mathbf{r}}_{ij} = \mathbf{r}_{ij}/r_{ij}$ with $r_{ij} = |\mathbf{r}_i - \mathbf{r}_j|$. The dissipative force is $\mathbf{F}^D_{ij} = -\gamma\omega^D(r_{ij})(\hat{\mathbf{r}}_{ij} \cdot \mathbf{v}_{ij})\hat{\mathbf{r}}_{ij}$ and the random force is $\mathbf{F}^R_{ij} = \sigma\omega^R(r_{ij})\xi_{ij}(dt)^{1/2}\hat{\mathbf{r}}_{ij}$, where $\mathbf{v}_{ij} = \mathbf{v}_i - \mathbf{v}_j$ and ξ_{ij} is a zero-mean Gaussian random variable of unit variance with $\xi_{ij} = \xi_{ji}$. The coefficients γ and $\sigma^2 = 2k_BT\gamma$ determine the strength of dissipative and random forces, where k_B is the Boltzmann constant and T is the temperature of the system. Moreover, the weight functions are $\omega^R(r_{ij}) = 1 - \hat{r}_{ij}$ and $\omega^D(r_{ij}) = [\omega^R(r_{ij})]^2$.[70] In our simulations, we set the time step $\Delta t = 0.01$, $m = 1$, $r_c = 1$, $\gamma = 4.5$, $a = 25$, $k_BT = 1$ and the number density $\rho = 3$ yielding the solvent kinematic viscosity ν equal to 0.283. Unless specified otherwise, all dimensional values are given in DPD units.

A random lattice of interconnecting elastic filaments[71] is used to model the capsule elastic shell. The flexible filaments are formed from DPD particles connected by Frankel springs with the potential $U_F = k_F(|\mathbf{r}_i - \mathbf{r}_j| - r_{eq})^2/2$. Here, we set the spring constant $k_F = 600$ and the equilibrium length $r_{eq} = 0.4$. The particles forming filaments also interact *via* DPD potentials. Additionally, we include a bending potential $U_b = k_b(1 + \cos\theta)$, where $k_b = 7.5$ is the bending stiffness and θ is the angle between two consecutive pairs of beads. This leads to filament bending rigidity $EI \approx 2.74$, for filaments with the effective radius equal to the Stokes−Einstein radius of DPD beads $R_{SE} \approx 0.209$.[72]

We build the shell network in two steps. We first randomly distribute N cross-linking nodes inside the computational domain and then connect each node with C_{ave} closest nodes.[29] We have recently used this model to examine transport through deformable polymer networks and found good agreement with the theory and experiments.[29] To create a spherical capsule, we generate a cubic network with a side equal to the outer capsule diameter and then remove the beads that are outside the capsule shell. Specifically, a $30 \times 30 \times 30$ cubic network, with $N = 12000$, $C_{ave} = 8$, and porosity $\varepsilon \approx 0.85$, was used to construct capsules with an outer radius $R_o = 15$ and a membrane thickness $b = 5$. With this network arrangement, the average filament length is about unity, which we found to be small enough to provide microgel network integrity and capsule stability in the simulated conditions. In experimental settings, the capsule integrity can be further enhanced by choosing polymers with different molecular weights.[24,50]

To model the swelling/deswelling of responsive capsules, we dynamically alter the length of network filaments by changing the effective equilibrium distance between DPD beads within each filament. This allows us to simulate the internal stresses that cause the network to shrink or expand. In this fashion, we

can accurately capture the volume transition in polymer networks (see Supporting Information). In experiments, the appearance of internal network stresses driving gel swelling and deswelling volume transitions can result from changes in the environmental conditions such as pH, salt concentration, temperature, light intensity, etc.[1−11]

To model network swelling in our simulations, we increase r_{eq} by 50% that results in a 50% increase in the capsule diameter (see Figure 2a,b). For modeling network deswelling, we simultaneously reduce the equilibrium length r_{eq} by 50% and the strength of DPD potentials between filament beads by 80%. This results in a 20% reduction in the outer diameter of the capsule (see Figures 2c,d).

To examine and quantify the particle release, we introduce 100 nanoparticles that are initially randomly distributed inside the capsule cavity. The rigid nanoparticles are constructed from 13 DPD beads arranged in hexagonal close-packed spherical aggregates that obey the rigid body dynamics and interact with the solvent and network *via* the DPD potentials. The Stokes−Einstein radius corresponding to the effective hydrodynamic radius of these aggregates is $R_p \approx 0.7$,[72] which is slightly larger than the mean membrane pore size in the unswollen initial capsule (Figure 4a).

To study the release of linear macromolecules, we load the microcapsule interior with 100 polymer chains. Each chain is formed from 10 DPD beads connected sequentially by finitely extensible nonlinear elastic (FENE) springs. The FENE potential is given by $U_{FENE} = -k_{FENE} r^2_{max} \log[1 - |\mathbf{r}_i - \mathbf{r}_j|^2/r^2_{max}]$, where $k_{FENE} = 10$ is the stretching constant and $r_{max} = 1.5$ is the maximum spring extension. The gyration radius of these chains representing their hydrodynamic radius is $R_g \approx 1$ as calculated using equilibrium simulations in pure solvent. Unlike the polymer network, the encapsulated linear macromolecules are insensitive to external stimuli.

To probe the effect of intercapsular microrods on the release from deswelling microcapsules, we introduce rods with length $L = 10$ and radius $R_{rod} = 2$ that are constructed by clustering DPD beads. The rods behave as rigid bodies and interact with the solvent network and nanoparticles *via* the DPD potentials.

We carry out the release simulations in a $50 \times 50 \times 50$ periodic box that contains a viscous DPD solvent, a polymeric microcapsule, and encapsulated nanoparticles/polymer chains (Figure 1). After an initial system equilibration, we change the filament equilibrium length to mimic the gel swelling/deswelling and then continue the simulations for 3×10^5 time steps.

Acknowledgment. Financial support from the Donors of the Petroleum Research Fund administered by the ACS and an ICAM Travel Award (H.M.) (NSF Grant No. DMR-0844115 through ICAM-I2CAM, 1 Shields Avenue, Davis, CA 95616) are gratefully acknowledged.

Supporting Information Available: Swelling kinetics of solid and hollow spherical capsules. This material is available free of charge *via* the Internet at http://pubs.acs.org.

REFERENCES AND NOTES

1. Kasi, R. M.; Ahn, S. K.; Kim, S. C.; Sharma, N.; Zhou, Y. X. Stimuli-Responsive Polymer Gels. *Soft Matter* **2008**, *4*, 1151–1157.
2. Stuart, M. A. C.; Huck, W. T. S.; Genzer, J.; Muller, M.; Ober, C.; Stamm, M.; Sukhorukov, G. B.; Szleifer, I.; Tsukruk, V. V.; Urban, M.; *et al*. Emerging Applications of Stimuli-Responsive Polymer Materials. *Nat. Mater.* **2010**, *9*, 101–113.
3. Urban, M. W.; Liu, F. Recent Advances and Challenges in Designing Stimuli-Responsive Polymers. *Prog. Polym. Sci.* **2010**, *35*, 3–23.
4. Peppas, N. A.; Hilt, J. Z.; Khademhosseini, A.; Langer, R. Hydrogels in Biology and Medicine: From Molecular Principles to Bionanotechnology. *Adv. Mater.* **2006**, *18*, 1345–1360.
5. Langer, R.; Tirrell, D. A. Designing Materials for Biology and Medicine. *Nature* **2004**, *428*, 487–492.
6. Kreft, O.; Javier, A. M.; Sukhorukov, G. B.; Parak, W. J. Polymer Microcapsules as Mobile Local pH-Sensors. *J. Mater. Chem.* **2007**, *17*, 4471–4476.
7. Park, K.; Qiu, Y. Environment-Sensitive Hydrogels for Drug Delivery. *Adv. Drug Delivery Rev.* **2001**, *53*, 321–339.
8. Olsson, R. T.; Samir, M. A. S. A.; Salazar-Alvarez, G.; Belova, L.; Strom, V.; Berglund, L. A.; Ikkala, O.; Nogues, J.; Gedde, U. W. Making Flexible Magnetic Aerogels and Stiff Magnetic Nanopaper Using Cellulose Nanofibrils as Templates. *Nat. Nanotechnol.* **2010**, *5*, 584–588.
9. Maeda, S.; Nakamaru, S.; Hara, Y.; Hashimoto, S. Control of Autonomous Swelling−Deswelling Behavior for a Polymer Gel. *J. Phys. Chem. B* **2009**, *113*, 4609–4613.
10. Gorelikov, I.; Field, L. M.; Kumacheva, E. Hybrid Microgels Photoresponsive in the Near-Infrared Spectral Range. *J. Am. Chem. Soc.* **2004**, *126*, 15938–15939.
11. Tomatsu, I.; Peng, K.; Kros, A. Photoresponsive Hydrogels for Biomedical Applications. *Adv. Drug Deliver. Rev.* **2011**, *63*, 1257–1266.
12. Zha, L. S.; Banik, B.; Alexis, F. Stimulus Responsive Nanogels for Drug Delivery. *Soft Matter* **2011**, *7*, 5908–5916.
13. Pavlov, A. M.; Sapelkin, A. V.; Huang, X. Y.; P'ng, K. M. Y.; Bushby, A. J.; Sukhorukov, G. B.; Skirtach, A. G. Neuron Cells Uptake of Polymeric Microcapsules and Subsequent Intracellular Release. *Macromol. Biosci.* **2011**, *11*, 848–854.
14. Bajpai, A. K.; Shukla, S. K.; Bhanu, S.; Kankane, S. Responsive Polymers in Controlled Drug Delivery. *Prog. Polym. Sci.* **2008**, *33*, 1088–1118.
15. Seiffert, S.; Thiele, J.; Abate, A. R.; Weitz, D. A. Smart Microgel Capsules from Macromolecular Precursors. *J. Am. Chem. Soc.* **2010**, *132*, 6606–6609.
16. Minko, S.; Tokarev, I. Stimuli-Responsive Porous Hydrogels at Interfaces for Molecular Filtration, Separation, Controlled Release, and Gating in Capsules and Membranes. *Adv. Mater.* **2010**, *22*, 3446–3462.
17. Gref, R.; Minamitake, Y.; Peracchia, M. T.; Trubetskoy, V.; Torchilin, V.; Langer, R. Biodegradable Long-Circulating Polymeric Nanospheres. *Science* **1994**, *263*, 1600–1603.
18. Skirtach, A. G.; Delcea, M.; Mohwald, H. Stimuli-Responsive LBL Capsules and Nanoshells for Drug Delivery. *Adv. Drug Delivery Rev.* **2011**, *63*, 730–747.
19. Xing, Z.; Wang, C.; Yan, J.; Zhang, L.; Li, L.; Zha, L. Dual Stimuli Responsive Hollow Nanogels with IPN Structure for Temperature Controlling Drug Loading and pH Triggering Drug Release. *Soft Matter* **2011**, *7*, 7992–7997.
20. Kent, S. J.; Sexton, A.; Whitney, P. G.; Chong, S. F.; Zelikin, A. N.; Johnston, A. P. R; De Rose, R.; Brooks, A. G.; Caruso, F. A Protective Vaccine Delivery System for *in Vivo* T Cell Stimulation Using Nanoengineered Polymer Hydrogel Capsules. *ACS Nano* **2009**, *3*, 3391–3400.
21. Skirtach, A. G.; Karageorgiev, P.; Bedard, M. F.; Sukhorukov, G. B.; Mohwald, H. Reversibly Permeable Nanomembranes of Polymeric Microcapsules. *J. Am. Chem. Soc.* **2008**, *130*, 11572–11573.
22. Hong, W.; Zhao, X. H.; Zhou, J. X.; Suo, Z. G. A Theory of Coupled Diffusion and Large Deformation in Polymeric Gels. *J. Mech. Phys. Solids* **2008**, *56*, 1779–1793.
23. Durbin, E. W.; Buxton, G. A. A Coarse-Grained Model of Targeted Drug Delivery from Responsive Polymer Nanoparticles. *Soft Matter* **2010**, *6*, 762–767.
24. Gao, C.; Donath, E.; Moya, S.; Dudnik, V.; Mohwald, H. Elasticity of Hollow Polyelectrolyte Capsules Prepared by the Layer-by-Layer Technique. *Eur. Phys. J. E* **2001**, *5*, 21–27.
25. Wahrmund, J.; Kim, J. W.; Chu, L. Y.; Wang, C. J.; Li, Y.; Fernandez-Nieves, A.; Weitz, D. A.; Krokhin, A.; Hu, Z. B. Swelling Kinetics of a Microgel Shell. *Macromolecules* **2009**, *42*, 9357–9365.
26. Tanaka, T.; Fillmore, D. J. Kinetics of Swelling of Gels. *J. Chem. Phys.* **1979**, *70*, 1214–1218.
27. We find that the network pore distributions for initial, swollen and deswollen gels are close to the Gaussian distribution, which is in agreement with the experimental data of ref 28.
28. Mickel, W.; Munster, S.; Jawerth, L. M.; Vader, D. A.; Weitz, D. A.; Sheppard, A. P.; Mecke, K.; Fabry, B.; Schroder-Turk, G. E. Robust Pore Size Analysis of Filamentous Networks from Three-Dimensional Confocal Microscopy. *Biophys. J.* **2008**, *95*, 6072–6080.

29. Masoud, H.; Alexeev, A. Permeability and Diffusion through Mechanically Deformed Random Polymer Networks. *Macromolecules* **2010**, *43*, 10117–10122.
30. We find that during swelling capsules temporarily loose their initially spherical shapes, which indicates a possible instability (buckling) caused by the rapid gel expansion. However, elastic forces in the membrane shell are sufficient to restore the nearly spherical shape after the equilibration of swollen capsules. The instability can be further mitigated by increasing the volume transition time.
31. Phillies, G. D. J. The Hydrodynamic Scaling Model for Polymer Self-Diffusion. *J. Phys. Chem.* **1989**, *93*, 5029–5039.
32. Phillies, G. D. J.; Pirnat, T.; Kiss, M.; Teasdale, N.; Maclung, D.; Inglefield, H.; Malone, C.; Rau, A.; Yu, L. P.; Rollings, J. Probe Diffusion in Solutions of Low-Molecular-Weight Polyelectrolytes. *Macromolecules* **1989**, *22*, 4068–4075.
33. Note that percolation through membranes can be characterized by an effective diffusion coefficient that is lower than the diffusion coefficient in unbounded networks due to an entropic barrier that prevents solute entrance into the network. This latter effect is more pronounced for flexible chains (see ref 34.).
34. Gam, S.; Meth, J. S.; Zane, S. G.; Chi, C. Z.; Wood, B. A.; Seitz, M. E.; Winey, K. I.; Clarke, N.; Composto, R. J. Macromolecular Diffusion in a Crowded Polymer Nanocomposite. *Macromolecules* **2011**, *44*, 3494–3501.
35. He, Q. J.; Guo, L. M.; Cui, F. M.; Chen, Y.; Jiang, P.; Shi, J. L. Facile One-Pot Synthesis and Drug Storage/Release Properties of Hollow Micro/Mesoporous Organosilica Nanospheres. *Mater. Lett.* **2009**, *63*, 1943–1945.
36. Zhu, Y. F.; Shi, J. L. A Mesoporous Core−Shell Structure for pH-Controlled Storage and Release of Water-Soluble Drug. *Microporous Mesoporous Mater.* **2007**, *103*, 243–249.
37. Zhu, Y. F.; Shi, J. L.; Shen, W. H.; Dong, X. P.; Feng, J. W.; Ruan, M. L.; Li, Y. S. Stimuli-Responsive Controlled Drug Release from a Hollow Mesoporous Silica Sphere/Polyelectrolyte Multilayer Core−Shell Structure. *Angew. Chem., Int. Ed.* **2005**, *44*, 5083–5087.
38. Kono, K.; Kimura, S.; Imanishi, Y. pH-Responsive Permeability of Polyamide Capsule Membrane Coated with Lipid Molecules and Amphiphilic Polypeptides. *J. Membr. Sci.* **1991**, *58*, 1–9.
39. Arifin, D. Y.; Lee, L. Y.; Wang, C. H. Mathematical Modeling and Simulation of Drug Release from Microspheres: Implications to Drug Delivery Systems. *Adv. Drug Delivery Rev.* **2006**, *58*, 1274–1325.
40. Hu, Z. B.; Zhang, X. M.; Li, Y. Synthesis and Application of Modulated Polymer Gels. *Science* **1995**, *269*, 525–527.
41. Li, Y.; Tanaka, T. Phase-Transitions of Gels. *Annu. Rev. Mater. Sci.* **1992**, *22*, 243–277.
42. Allan, S, H. Applications of Thermally Reversible Polymers and Hydrogels in Therapeutics and Diagnostics. *J. Controlled Release* **1987**, *6*, 297–305.
43. Okano, T.; Kikuchi, A. Pulsatile Drug Release Control Using Hydrogels. *Adv. Drug Delivery Rev.* **2002**, *54*, 53–77.
44. Yoshida, R.; Sakai, K.; Okano, T.; Sakurai, Y. Pulsatile Drug-Delivery Systems Using Hydrogels. *Adv. Drug Delivery Rev.* **1993**, *11*, 85–108.
45. Patel, D.; Patel, B.; Patel, C. An Overview on Intelligent Drug Delivery Systems. *Int. J. Adv. Pharm. Res.* **2011**, *2*, 57–63.
46. Zha, L. S.; Zhang, Y.; Yang, W. L.; Fu, S. K. Monodisperse Temperature-Sensitive Microcontainers. *Adv. Mater.* **2002**, *14*, 1090–1092.
47. Zhang, Y. J.; Guan, Y.; Zhou, S. Q. Synthesis and Volume Phase Transitions of Glucose-Sensitive Microgels. *Biomacromolecules* **2006**, *7*, 3196–3201.
48. Koo, H. Y.; Chang, S. T.; Choi, W. S.; Park, J. H.; Kim, D. Y.; Velev, O. D. Emulsion-Based Synthesis of Reversibly Swellable, Magnetic Nanoparticle-Embedded Polymer Microcapsules. *Chem. Mater.* **2006**, *18*, 3308–3313.
49. Motornov, M.; Royter, H.; Lupitskyy, R.; Roiter, Y.; Minko, S. Stimuli-Responsive Hydrogel Hollow Capsules by Material Efficient and Robust Cross-Linking-Precipitation Synthesis Revisited. *Langmuir* **2011**, *27*, 15305–15311.
50. Fery, A.; Dubreuil, F.; Mohwald, H. Mechanics of Artificial Microcapsules. *New. J. Phys.* **2004**, *6*, 18.
51. Zahr, A. S.; de Villiers, M.; Pishko, M. V. Encapsulation of Drug Nanoparticles in Self-Assembled Macromolecular Nanoshells. *Langmuir* **2005**, *21*, 403–410.
52. Wang, Y. J.; Yan, Y.; Cui, J. W.; Hosta-Rigau, L.; Heath, J. K.; Nice, E. C.; Caruso, F. Encapsulation of Water-Insoluble Drugs in Polymer Capsules Prepared Using Mesoporous Silica Templates for Intracellular Drug Delivery. *Adv. Mater.* **2010**, *22*, 4293–4297.
53. Kozlovskaya, V.; Kharlampieva, E.; Mansfield, M. L.; Sukhishvili, S. A. Poly(Methacrylic Acid) Hydrogel Films and Capsules: Response to pH and Ionic Strength, and Encapsulation of Macromolecules. *Chem. Mater.* **2006**, *18*, 328–336.
54. Kim, S. H.; Hwang, H.; Lim, C. H.; Shim, J. W.; Yang, S. M. Packing of Emulsion Droplets: Structural and Functional Motifs for Multicored Microcapsules. *Adv. Funct. Mater.* **2011**, *21*, 1608–1615.
55. Shum, H. C.; Zhao, Y. J.; Kim, S. H.; Weitz, D. A. Multicompartment Polymersomes from Double Emulsions. *Angew. Chem., Int. Ed.* **2011**, *50*, 1648–1651.
56. Dahne, L.; Leporatti, S.; Donath, E.; Mohwald, H. Fabrication of Microreaction Cages with Tailored Properties. *J. Am. Chem. Soc.* **2001**, *123*, 5431–5436.
57. Vriezema, D. M.; Aragones, M. C.; Elemans, J. A. A. W.; Cornelissen, J. J. L. M.; Rowan, A. E.; Nolte, R. J. M. Self-Assembled Nanoreactors. *Chem. Rev.* **2005**, *105*, 1445–1489.
58. Xing, Z. M.; Wang, C. L.; Yan, J.; Zhang, L.; Li, L.; Zha, L. S. Dual Stimuli Responsive Hollow Nanogels with IPN Structure for Temperature Controlling Drug Loading and pH Triggering Drug Release. *Soft Matter* **2011**, *7*, 7992–7997.
59. Hoogerbrugge, P. J.; Koelman, J. M. V. A. Simulating Microscopic Hydrodynamic Phenomena with Dissipative Particle Dynamics. *Europhys. Lett.* **1992**, *19*, 155–160.
60. Groot, R. D.; Warren, P. B. Dissipative Particle Dynamics: Bridging the Gap between Atomistic and Mesoscopic Simulation. *J. Chem. Phy.* **1997**, *107*, 4423–4435.
61. Groot, R. D.; Rabone, K. L. Mesoscopic Simulation of Cell Membrane Damage, Morphology Change and Rupture by Nonionic Surfactants. *Biophys. J.* **2001**, *81*, 725–736.
62. Alexeev, A.; Uspal, W. E.; Balazs, A. C. Harnessing Janus Nanoparticles To Create Controllable Pores in Membranes. *ACS Nano* **2008**, *2*, 1117–1122.
63. Masoud, H.; Alexeev, A. Selective Control of Surface Properties Using Hydrodynamic Interactions. *Chem. Commun.* **2011**, *47*, 472–474.
64. Yan, L. T.; Popp, N.; Ghosh, S. K.; Boker, A. Self-Assembly of Janus Nanoparticles in Diblock Copolymers. *ACS Nano* **2010**, *4*, 913–920.
65. Yan, L. T.; Yu, X. B. Enhanced Permeability of Charged Dendrimers across Tense Lipid Bilayer Membranes. *ACS Nano* **2009**, *3*, 2171–2176.
66. Dutt, M.; Kuksenok, O.; Nayhouse, M. J.; Little, S. R.; Balazs, A. C. Modeling the Self-Assembly of Lipids and Nanotubes in Solution: Forming Vesicles and Bicelles with Transmembrane Nanotube Channels. *ACS Nano* **2011**, *5*, 4769–4782.
67. Karniadakis, G. E.; Fedosov, D. A.; Pan, W. X.; Caswell, B.; Gompper, G. Predicting Human Blood Viscosity in Silico. *Proc. Natl. Acad. Sci. U.S.A.* **2011**, *108*, 11772–11777.
68. Zerbetto, F.; Calvaresi, M.; Dallavalle, M. Wrapping Nanotubles with Micelles, Hemimicelles, and Cylindrical Micelles. *Small* **2009**, *5*, 2191–2198.
69. Rodriguez-Hidalgo, M.-d.-R.; Soto-Figueroa, C.; Vicente, L. Mesoscopic Simulation of the Drug Release Mechanism on the Polymeric Vehicle P(ST-DVB) in an Acid Environment. *Soft Matter* **2011**, *7*, 8224–8230.
70. Espanol, P.; Warren, P. Statistical-Mechanics of Dissipative Particle Dynamics. *Europhys. Lett.* **1995**, *30*, 191–196.
71. Buxton, G. A.; Clarke, N. "Bending to Stretching" Transition in Disordered Networks. *Phys. Rev. Lett.* **2007**, *98*, 238103.
72. Pan, W. X.; Fedosov, D. A.; Karniadakis, G. E.; Caswell, B. Hydrodynamic Interactions for Single Dissipative-Particle-Dynamics Particles and Their Clusters and Filaments. *Phys. Rev. E* **2008**, *78*, 46706.